Published in final edited form as:
Free Radic Biol Med. 2008 March 1; 44(5): 868–881. doi:10.1016/j.freeradbiomed.2007.11.020.

NOVEL REDOX-DEPENDENT REGULATION OF NOX5 BY THE TYROSINE KINASE C-ABL

Amina El Jamali[a,*], **Anthony J. Valente**[a], **James D. Lechleiter**[b], **Maria J. Gamez**[a], **Doran W. Pearson**[a], **William M. Nauseef**[c], and **Robert A. Clark**[a]

a *Departments of Medicine, University of Texas Health Science Center, and South Texas Veterans Health Care System, Audie L. Murphy Division, San Antonio, Texas 78229-3900 USA*

b *Departments of Cellular and Structural Biology, University of Texas Health Science Center, and South Texas Veterans Health Care System, Audie L. Murphy Division, San Antonio, Texas 78229-3900 USA*

c *Inflammation Program, Department of Medicine, the University of Iowa And Veterans Administration Medical Center, Iowa City, IA 52241 USA*

Abstract

We investigated the mechanism of H_2O_2 activation of the Ca^{2+}-regulated NADPH oxidase NOX5. H_2O_2 induced a transient, dose-dependent increase in superoxide production in K562 cells expressing NOX5. Confocal studies demonstrated that the initial calcium influx generated by H_2O_2 is amplified by a feedback mechanism involving NOX5-dependent superoxide production and H_2O_2. H_2O_2-NOX5 activation was inhibited by extracellular Ca2+ chelators, a pharmacological inhibitor of c-Abl, and over-expression of kinase-dead c-Abl.

Transfected kinase-active GFP-c-Abl co-localized with vesicular sites of superoxide production in a Ca^{2+}-dependent manner. In contrast to H_2O_2, the Ca2+ ionophore ionomycin induced NOX5 activity independently of c-Abl. Immunoprecipitation of cell lysates revealed that active GFP-c-Abl formed oligomers with endogenous c-Abl and that phosphorylation of both proteins was increased by H_2O_2 treatment. Furthermore, H_2O_2-induced NOX5 activity correlated with increased localization of c-Abl to the membrane fraction, and NOX5 proteins could be co-immunoprecipitated with GFP-Abl proteins.

Our data demonstrate for the first time that NOX5 is activated by c-Abl through a Ca^{2+}-mediated, redox-dependent signaling pathway and suggest a functional association between NOX5 NADPH oxidase and c-Abl.

Keywords

NADPH oxidase; NOX5; hydrogen peroxide; signaling; c-Abl; superoxide; calcium

* Corresponding author: Department of Medicine/Infectious Diseases, University of Texas Health Science Center, 7703 Floyd Curl Drive, San Antonio, Texas 78229-3900 USA, Tel: 210-567-1992; Fax: 210-567-4654; E-mail: AkoulouzeBik@uthscsa.edu.

Introduction

Reactive oxygen species (ROS) are now recognized as physiologically relevant mediators of both host defense and cell signaling. There is growing evidence that the transient production of hydrogen peroxide (H_2O_2) is an important signaling event triggered by the interaction of a variety of cell surface receptors with their ligands [1–7] and that NADPH oxidases (NOX) are prominent sources of receptor-activated H_2O_2 [8].

NADPH oxidases reduce molecular oxygen to superoxide, which undergoes dismutation, either spontaneously or catalytically, to form H_2O_2. Seven members of the *NOX* gene family have been identified [9–11], each with characteristic tissue distribution, putative function, and regulation. All members share common structural characteristics, including six hydrophobic transmembrane domains, conserved motifs in the cytoplasmic domains involved in NADPH and FAD binding, and two heme moieties, which are localized to the intra-membranous domain [9–11]. In addition to these common features, NADPH oxidase 5 (NOX5) contains an N-terminal extension with four Ca^{2+}-binding EF hand domains [12]. While NOX1, NOX2 and NOX3 require cytosolic subunits and co-factors to display full activity, it appears that NOX5 can be activated by Ca^{2+} alone [13].

Since H_2O_2 affects many proteins potentially involved in the regulation of NADPH oxidase activity [14,15], we hypothesized that it may regulate its own production by stimulating NOX activity. Such a positive feedback mechanism, in either autocrine or paracrine mode, might amplify the receptor response to its specific ligand by enhancing recruitment of signaling intermediates. Such regulation has been recently described for NOX2 in interleukin 1 signaling [16]. Here we report for the first time activation of NOX5 by H_2O_2 through a novel pathway featuring Ca^{2+}-mediated redox-dependent regulation of the non-receptor tyrosine kinase c-Abl.

Experimental Procedures

Cell culture and stable expression of NOX5 and Abl proteins in K562 cells

K562 human leukemia cells were grown in RPMI medium supplemented with 10% fetal bovine serum, plus 100 U/ml penicillin and 100 μg/ml streptomycin. Cells in the logarithmic phase of growth were transfected with expression vectors as described previously [17] and stable expressing clones selected in the appropriate antibiotic. Single cell clones were established by limiting dilution in 96-well plates. The human NOX5β cDNA cloned into pGEX-2T vector and the HEK293 cell line stably expressing the NOX5 protein were kindly provided by Botond Banfi, University of Iowa. [12]. NOX5 subcloned in pcDNA3.1 and pRep4 were used to generate stable NOX5-expressing K562 cells. The pcDNA 3.1 expression vector encoding the GFP-tagged wild-type Abl (full-length, isoform Ib, GFP-c-Abl) and the GFP-tagged kinase-dead (KD) K290R mutant of c-Abl (GFP-KD-c-Abl) were kindly provided by Z.-M. Yuan, Harvard School of Public Health [18]. NOX5 protein was detected by immunoblot using a rabbit polyclonal NOX5 antibody raised against a fusion protein containing the EF hand domain (amino acids 1–169). Expression of GFP-c-Abl and GFP-KD-c-Abl was documented by fluorescence microscopy. For experiments with GFP-c-Abl or GFP-KD-c-Abl, K562 cells stably expressing these proteins were transfected with NOX5β/pREP4 and selected in hygromycin (400 μg/ml).

Cell Treatment

K562 cells were treated for 30 minutes at 37°C with either vehicle or inhibitors of PI3-kinase (10 μM LY294002, Calbiochem), src family kinases (10 μM Genistein, Sigma), protein phosphatases (1 mM sodium orthovanadate, Sigma), SERCA Ca^{2+} pumps (100 nM thapsigargin, EMD Bioscience). Overnight treatment was used for the c-Abl tyrosine kinase

inhibitor imatinib mesylate (10 μM, Novartis Pharma AG, Basel, Switzerland). In Ca^{2+} chelation studies, cells were suspended in PBS-G (phosphate buffered saline with 10 mM glucose) supplemented with BAPTA (50 μM) for 5 minutes, followed by washing in PBS-G or PBS-G containing BAPTA, and stimulation with 100 μM H_2O_2 for 10 minutes at 37°C. The vehicles used in the pharmacological studies, DMSO and ethanol, had no effect on superoxide production (Supplement Figure 1).

Subcellular fractionation

Cell lysis was carried out in buffer A (20 mM HEPES, pH 7.9; 350 mM NaCl; 0.5 mM EDTA; 0.5 mM EGTA; 1 mM $MgCl_2$; 10% glycerol; 1% Nonidet P-40; 10 mM NaF; 0.1 mM Na_3VaO_4 [orthovanadate], 8 mM β-glycerophosphate; phosphatase inhibitor cocktail I and II [Sigma]; and protease inhibitor cocktail [Roche, Mannheim, Germany]). Lysates were cleared by centrifugation and, where indicated, the protein extracts were centrifuged at 100,000 g for 1 hour to separate the crude membranes from the cytosolic proteins. Protein content was estimated as described [19].

Superoxide assay on whole cells

Superoxide generation was measured using a luminol-based chemiluminescence assay (Diogenes). Cells were collected by centrifugation, washed once in PBS, resuspended at 5×10^6/ml in PBS-G, and kept on ice until assayed. For the assay, a 100 μl aliquot of the Diogenes reagent was mixed with a maximum of 0.5×10^6 cells and incubated at 37°C for 2–4 minutes. Superoxide generation was stimulated with H_2O_2 (100 μM) or ionomycin (100 nM). Chemiluminescence was measured every 30–60 seconds for up to 10 minutes using a Turner Designs 20/20 luminometer and an integration time of 5 seconds. The conditions used for the superoxide assay are within the linear range of detection as shown in Supplement Figure 2.

Superoxide assay on crude membrane preparation

Reaction mixtures contained 0.2X PBS, pH 7.5, 10 μM FAD, 0.3 mM BAPTA, 0.3 mM EDTA, 0.3 mM nitrilotriacetic acid, 1 mM $MgCl_2$, 5.5 μM phosphatidic acid (1,2 didecanoyl-sn-glycerol-3-phosphate, Sigma), 0.65 mM $CaCl_2$ (corresponding to an estimated free Ca^{2+} concentration of 47 μM using the WEBMAXC STANDARD software), 0 or 400 units/ml superoxide dismutase (SOD from bovine erythrocytes, Sigma), and 50 to 100 μg/ml of membrane protein. Superoxide production was initiated by the addition of 200 μM NADPH and quantitated using the Diogenes reagent when H_2O_2 was added to the reaction mixture. In the pabsence of H_2O_2, the superoxide production was also determined by the SOD-inhibitable reduction of cytochrome c (100 μM) and absolute amounts calculated using $\Delta\varepsilon 550 = 21{,}000$ M^{-1} cm^{-1} as extinction coefficient of the reduced cytochrome [20]. Average rates of superoxide generation were calculated from the linear region of the absorbance curve and expressed as pmol of $O_2^{\bullet -}$/minute/mg of membrane protein.

Immunoprecipitation and immunoblot analysis

Total cell extracts prepared in buffer A (250 μg of protein) were pre-cleared with rabbit IgG and protein A/G -Agarose (Santa Cruz), incubated overnight with anti-GFP antibody (Molecular Probes), and precipitated with protein A/G-Agarose for an additional 3 hours. The immune complexes were washed with lysis buffer, separated on 4–20% SDS polyacrylamide gradient gels and transferred to polyvinylidene difluoride (PVDF) membranes. The filters were incubated monoclonal anti-c-Abl antibody (clone ABL-148, Sigma), anti-phosphotyrosine (clone 4G10; Upstate/Millipore) or with the rabbit polyclonal NOX5 antibody described above. In some immunoblots, antibody to protein disulfide isomerase (PDI, EMD Biosciences) was used as a loading control. The antigen-antibody complexes were visualized by enhanced chemiluminescence (ECL, Amersham Corp.).

Difference spectroscopy

Membrane fractions collected by ultracentrifugation of cell lysates at 100,000 g for 1 hour were resuspended in PBS consisting of 2.7 mM KCl, 136.7 mM NaCl, 1.5 mM KH_2PO_4, and 8.1 mM Na_2HPO_4, pH 7.4, supplemented with a cocktail of protease inhibitors (Roche) and 1 mM EDTA. The difference spectra of dithionite reduced minus oxidized samples were recorded at room temperature for membranes isolated from either K562 cells or K562 cells expressing NOX5 [21].

Live Cell Imaging

K562 cells were washed x3 in PBS-G and plated on poly L-lysine-coated glass coverslips for 60 minutes (3×10^5 cells/ml) in complete RPMI medium without phenol red. Where indicated, the cells were loaded with 6 μM fluo4-AM (Molecular Probes) for 15 minutes and washed x3 in PBS-G to remove free probe. The cells were then incubated in complete medium supplemented with 10 mM HEPES without phenol red for an additional 15 minutes at 37°C to allow de-esterification of the probe. At 15 minutes before imaging, the cells were incubated with 300 nM hydroethidine (HE) (Molecular Probes). Ca^{2+} influx and superoxide production were recorded as indicated in the figure legends. For the detection and localization of GFP-tagged Abl proteins the same procedure was used, except that no fluo4-AM was added. For HEK293 cells expressing NOX5 (HEK/NOX5) the same loading protocol with the fluorescent probes was used. Live cell imaging was performed using a confocal microscope (LSM 510; Carl Zeiss MicroImaging, Inc.) with a 63X/1.4 NA plan-apochromat objective. Fluo-4 or GFP and HE fluorescence were excited with an Argon laser (488 nm) attenuated to avoid photobleaching and saturation. Simultaneous detection was through a 545 nm long-pass dichroic mirror and a band-pass filter at 500–530 for fluo-4 or GFP fluorescence and LP560 for HE fluorescence. Image acquisition of the fluorescence intensity was performed with the Zeiss LSM510 Software 3.2 SP2. The pinhole was opened to 1 Airy unit and time lapse images were collected at 20 second intervals for up to 30 minutes. Similar experiments were performed using dual excitation at 488/543nm. Results using the single excitation at 488 or the dual excitation 488/543nm gave the same pattern of results. Intensity measurements of the fluorescent signals were analyzed using ImageJ software.

Statistical analysis

Data are presented as the mean ± SEM of the values and were normalized to controls. Statistical analysis was performed using mainly the Dunnett multiple comparisons test to adjust for multiple testing when comparing several means against the mean for a common control sample. The Tukey multiple comparison procedure was used to adjust for multiple testing other pair-wise comparisons among several means. A value for $P < 0.05$ was accepted as significant.

Results

Hydrogen peroxide induces NOX5 activity

To study the effect of H_2O_2 on NOX5 activity, we used K562 human myeloid cells ectopically expressing the NOX5 protein (K562/NOX5 cells). Immunoblotting with NOX5 antibody demonstrated a band of ~75kDa in the crude membranes of K562/NOX5 cells, but not the K562 parental line (Fig. 1A).

The luminol-based chemiluminescence assay (Diogenes® reagent) was used to measure the effect of H_2O_2 on NOX5 activity, since this reagent selectively detects superoxide anion. We confirmed that this reagent does not react with H_2O_2 by testing the effect of H_2O_2 addition on the generation of superoxide by the xanthine-xanthine oxidase reaction (Supplement Fig. 3). H_2O_2 at the concentrations used in this study (100 μM), had no effect on the measured output

of this system. Furthermore, the addition of H_2O_2 at these concentrations had no effect on the very low levels of chemiluminescence generated by the parental K562 cells (Fig. 1B, 1C), suggesting that the superoxide generated in K562/NOX5 cells in response to H_2O_2 is primarily dependent on the NOX5 protein (Fig. 1D, E, F). Furthermore, all chemiluminescence detected by the Diogenes® reagent was abrogated by the addition of superoxide dismutase (SOD) (Supplement Fig. 3), indicating that generation of superoxide anion was being specifically detected.

In K562/NOX5 cells, H_2O_2 induced a marked burst in superoxide production, with maximal activity observed 5–10 minutes after peroxide addition (Fig. 1D). This induction of NOX5-dependent superoxide production was dose-dependent with a 10 to 20-fold increase exhibited at 100 μM H_2O_2 (Fig. 1E). Under these conditions, no detectable effect on cell viability was observed using the trypan blue exclusion assay (data not shown). The response to H_2O_2 was completely abrogated by the addition of catalase (Fig. 1F).

H_2O_2 does not activate NOX5 NADPH oxidase by a direct effect on NOX5 protein

Since NOX5 functions independently of cytosolic co-factor proteins [13], we were able to investigate whether H_2O_2 directly stimulated NOX5 by using membranes prepared from NOX5-expressing K562 cells. To detect the presence of NOX5, we compared the absorption spectra of dithionite-reduced versus oxidized membranes prepared from parental K562 and K562/NOX5 cells. Absorbance peaks at 425 and 558 nm, characteristic of cytochrome b_{558}, were observed only in the membranes of the K562/NOX5 cells (Fig. 2A).

Using the chemiluminescence assay, no superoxide production was detected in control K562 membranes in the presence of Ca^{2+} and NADPH (Fig. 2B). On the other hand, membranes from K562/NOX5 cells exhibited a robust chemiluminescent response that was dependent on both Ca^{2+} and NADPH, but inhibited by either SOD or diphenylene iodonium (DPI). The response was not inhibited by azide (Fig. 2B), a hallmark of NOX proteins [22]. The effect of H_2O_2 was tested in the presence of various concentrations of free Ca^{2+} [0–800μM]. In contrast to the effect on intact cells and for all free Ca^{2+} concentrations tested, 100 μM H_2O_2 did not stimulate superoxide production in the K562/NOX5 membranes (Fig. 2C). These results suggestthat the H_2O_2-induced superoxide generation observed in intact K562/NOX5 cells is unlikely due to a direct effect of H_2O_2 on the NOX5 protein *per se*.

Role of Ca^{2+} signaling and tyrosine kinases in H_2O_2-NOX5 regulation

Since H_2O_2 is reported to regulate a broad range of signaling proteins [23,24], we next studied the effect of inhibitors of various signaling pathways on the activation of NOX5-dependent superoxide production. Inhibitors of MEK1/2 (U0126), protein kinase A (H89), and phospholipase A_2 did not block the induction of NOX5 activity by H_2O_2 (data not shown), nor did inhibitors of phosphatidyl inositol 3-kinase (LY294002) and protein phosphatases (orthovanadate) (Fig. 3). We then investigated pathways involving Ca^{2+}, the major activator of NOX5, and tyrosine kinases, which have been reported to be involved in H_2O_2 signaling [1,5]. K562/NOX5 cells were pre-treated with either genistein, an inhibitor of the src family tyrosine kinases, imatinib mesylate, an inhibitor of Abl tyrosine kinase, thapsigargin, an inhibitor of sarco-endoplasmic reticulum Ca^{2+}-ATPase (SERCA), or with the extracellular Ca^{2+} chelator BAPTA, and then assayed for superoxide production (Fig. 3). H_2O_2-induced NOX5-dependent superoxide production was inhibited by the addition of BAPTA to the extracellular medium, but not by pretreatment with thapsigargin, which depletes endoplasmic reticulum Ca^{2+} stores and increases cytoplasmic Ca^{2+} (Fig. 3). However, in thapsigargin-treated cells, we did observe an increase of both basal and H_2O_2-stimulated NOX5-dependent superoxide production. These results suggest overall that influx of Ca^{2+} from the extracellular milieu, rather than from intracellular stores, is involved in H_2O_2 regulation of NOX5.

Furthermore, both the general src tyrosine kinase inhibitor, genistein, and the selective c-Abl inhibitor imatinib mesylate inhibited NOX5 stimulation by H_2O_2 (Fig. 3). We concluded from these studies that H_2O_2-induced NOX5-dependent superoxide production is mediated through pathways involving calcium influx and tyrosine kinase activity. Since the regulation of NOX5 by calcium is well documented, our subsequent studies were focused on the potential role and mechanism of activation of NOX5 by Abl tyrosine kinase.

A role for c-Abl in H_2O_2-mediated NOX5 activation

K562 cells express both native c-Abl and Bcr-Abl, the product of the t(9;22)(q34;q11) translocation fusing *BCR* gene sequences to the *ABL* proto-oncogene. Depending on where in the *BCR* locus the breakpoint occurs, either a 190 or a 210 kDa chimeric Bcr/Abl oncoprotein is produced. N-terminal Bcr sequences are directly responsible for the activation of the Abl tyrosine kinase in the chimeric Bcr/Abl gene products [25]. Bcr-Abl and c-Abl are both inhibited by imatinib mesylate [26]. Therefore, to define the specific role of c-Abl tyrosine kinase in H_2O_2-NOX5 activation, we used K562 cell lines stably over-expressing either GFP-tagged wild-type c-Abl (GFP-c-Abl), or GFP-tagged kinase-dead c-Abl (GFP-KD-c-Abl). Over-expression of GFP-c-Abl significantly enhanced both basal and H_2O_2-induced activity of NOX5 (Fig. 4A). In contrast, over-expression of the inactive GFP-KD-c-Abl had little effect on the basal activity of NOX5, but markedly inhibited the response to H_2O_2 (Fig. 4A). Furthermore, in Bcr-Abl-negative HEK cells stably expressing the NOX5 protein (Supplement Fig. 4), and transiently transfected with either control vector or the vectors encoding GFP-c-Abl or GFP-KD-c-Abl, the stimulation of NOX5 by H_2O_2 was also inhibited by kinase-dead, but not wild type c-Abl (Fig. 4B). Together with the previous data, these results strongly suggest that c-Abl is an important mediator of H_2O_2-induced NOX5 activity.

Amplification of H_2O_2-dependent Ca2+ influx by H_2O_2-dependent NOX5 activation

The role of Ca^{2+} and c-Abl in H_2O_2-NOX5 regulation was further investigated by confocal microscopy. To image cytosolic Ca^{2+} responses and superoxide production during H_2O_2 exposure, K562/NOX5 or K562 cells were loaded with the red fluorescent superoxide indicator hydroethidine (HE) and the Ca^{2+} indicator dye fluo4-AM. Control K562 cells stimulated by H_2O_2 or unstimulated K562/NOX5 cells both generated only low diffuse red fluorescence over time, suggesting a low level of superoxide production induced by the light excitation itself (Fig. 5B). When K562/NOX5 cells were exposed to H_2O_2 the emission of red fluorescence was significantly increased (Fig. 5A and B). Red fluorescence signals were detected at the plasma membrane and in discrete intracellular vesicles networking with the plasma membrane, and signals in both sites were abrogated by SOD and DPI (Fig. 5A), indicating that NOX5-dependent superoxide production was induced by H_2O_2 treatment.

Ca^{2+}-dependent fluo-4 fluorescence was observed in the cytoplasmic compartment, as well as in the vesicular sites of NOX5 superoxide production. Accumulation of dyes in cellular compartments is known to occur under some loading conditions, especially over prolonged periods [27]. In fact, an increased number of vesicles containing the fluo-4 dye were seen in both HEK/NOX5 cells (Fig. 5C) and K562/NOX5 cells (data not shown) as the time of incubation with the probe increased. The kinetics observed for the calcium influx appear to be multiphasic (Fig. 5B). An initial phase in response to H_2O_2 stimulation (0 to ~300 seconds) was observed in both K562 and K562/NOX5 cells. This initial calcium influx decayed rapidly in the K562 cells. In contrast, the calcium influx in the K562/NOX5 cells was dramatically increased over the same time period. This later phase of the calcium influx (~300–800 seconds) appeared to be dependent on the production of superoxide by NOX5, since it was only observed in stimulated K562/NOX5 cells and was significantly reduced by DPI and SOD (Fig. 5A). Since exogenous SOD is restricted to the extracellular medium, our results suggest that i) the early events leading to superoxide production occurred at the plasma membrane level, and ii)

superoxide itself is involved in the H_2O_2 signaling described. As expected, the addition of BAPTA to the extracellular medium profoundly reduced the effect of H_2O_2 on the fluorescence resulting from both Ca^{2+} influx and superoxide production. These results suggest coordination between calcium influx and superoxide production leading to an amplification loop system (cf. model Fig. 9). HEK/NOX5 cells demonstrated the same pattern as K562/NOX5 cells (Fig. 5C), except that both events took place at a slower rate.

Ca^{2+}-dependent relocalization of c-Abl is involved in H_2O_2-NOX5 activation

Since c-Abl was required for NOX5 activation by H_2O_2, we investigated the effect of H_2O_2 on the localization of c-Abl and superoxide production. In unstimulated cells, the GFP-tagged Abl proteins were mainly localized to the cytoplasmic compartment. However, following treatment with H_2O_2 for 10 minutes, the active GFP-c-Abl protein was redistributed into small vesicles, where a red signal, corresponding to superoxide production, was also observed (Fig. 6A, left panels). In the presence of 50 μM BAPTA, superoxide production and the redistribution of c-Abl were effectively abolished. In cells treated with imatinib or over-expressing the inactive GFP-KD-c-Abl, neither superoxide production nor c-Abl relocalization into vesicles was observed after treatment with H_2O_2 (Fig. 6A, right panels). These results suggest that H_2O_2-induced NOX5 activation involves the relocalization of c-Abl from the cytosolic compartment to the vesicles. This relocalization is dependent on both calcium influx and functional c-Abl. Interestingly, although the GFP-KD-c-Abl/NOX5 K562 cells were unresponsive to 100 μM H_2O_2; they still produced superoxide following treatment with the Ca2+ ionophore ionomycin (Fig. 6B) or with 10- to 100-fold higher concentration of H_2O_2 (Supplement Fig. 5). The level of superoxide detected was, however, higher in ionomycin-treated cells than in cells treated with 10mM H_2O_2. Furthermore, using the Diogenes reagent we observed that NOX5-dependent superoxide production induced by ionomycin was unaffected by 100 μM H_2O_2 treatment and/or the over-expression of wild-type or kinase-dead c-Abl (Fig. 6C). These results indicate that NOX5 is activated directly by high fluxes of Ca^{2+} in a c-Abl-independent manner, whereas regulation of NOX5 by 100 μM H_2O_2 requires a Ca^{2+}/c-Abl pathway. To our knowledge, this is the first description of a regulatory mechanism involving Ca^{2+}-dependent subcellular redistribution of c-Abl.

Tyrosine phosphorylation of c-Abl is a prerequisite for NOX5 regulation by H_2O_2

Since H_2O_2 has been reported to increase c-Abl tyrosine phosphorylation, thereby activating its tyrosine kinase activity [28,29], we investigated whether the Abl proteins in K562 cells were phosphorylated following H_2O_2 treatment. K562 cells expressing GFP-tagged Abl protein were pre-incubated with or without H_2O_2, and cell lysates were immunoprecipitated with anti-GFP antibodies and then immunoblotted with antibodies to phosphotyrosine and to c-Abl (Fig. 7). With the c-Abl antibodies (Fig. 7A), two bands were detected. These bands, which were not detectable in immunoprecipitates of K562 cells expressing only NOX5 protein, corresponded by molecular mass to the GFP-tagged Abl proteins (~160 kDa) and endogenous c-Abl (~130 kDa). The endogenous c-Abl protein was very prominent in the GFP-immunoprecipitates of cells over-expressing GFP-c-Abl, whereas it was found in only trace amounts in cells over-expressing GFP-KD-c-Abl. These results are consistent with earlier reports showing the oligomerization of over-expressed c-Abl proteins in COS cells [30]. This oligomerization exhibited variable stoichiometry, since the ratio of GFP-c-Abl protein/endogenous c-Abl ranged from about 1:2 to 1:5, depending of the experiment. This result does not reflect an increased expression of endogenous c-Abl in K562/NOX5 cells over-expressing the GFP-tagged proteins (Supplement Fig. 4). Interestingly, we did not detect a co-immunoprecipitating band corresponding to Bcr-Abl (210 kDa), which is the dominant Abl species in K562 cells, as shown in Supplement Figure 4. This result strongly suggests that the interaction with GFP-c-Abl was specific for endogenous c-Abl. In cells transfected with GFP-c-Abl, H_2O_2 increased tyrosine phosphorylation of both endogenous and GFP-tagged c-Abl.

In contrast, in cells over-expressing GFP-KD-c-Abl, the small amount of tyrosine phosphorylated GFP-KD-c-Abl observed was not regulated by H_2O_2, nor was tyrosine-phosphorylated endogenous c-Abl detected (Fig. 7A).

Interestingly, neither c-Abl tyrosine phosphorylation nor the co-immunoprecipitation of GFP-c-Abl with endogenous c-Abl was affected by BAPTA (Fig. 7B). Together with the confocal microscopy experiments, these immunoblotting studies suggest that H_2O_2 regulates c-Abl in a complex manner involving tyrosine phosphorylation, oligomerization, and redistribution of Abl protein to a specific membrane compartment. In this process, oligomerization and tyrosine-phosphorylation of Abl proteins requires an active kinase domain, but is independent of Ca^{2+}. Thus, Ca^{2+} appears to be selectively involved in the subcellular redistribution of kinase-active Abl proteins to the proper membrane compartment.

c-Abl interacts functionally with NOX5

To investigate whether c-Abl interacts functionally with NOX5, we measured NOX5 activity in crude membrane preparations from cells over-expressing wild-type or kinase-dead GFP-c-Abl. First, we analyzed whether Abl proteins were interacting with NOX5 proteins by performing a co-immunoprecipitation experiment. NOX5 protein was found in GFP-immunoprecipitates from lysate of K562/NOX5 cells over-expressing GFP-c-Abl (Fig. 8A, 8B), as well as in c-Abl immunoprecipitates from HEK/NOX5 cells (Fig. 8C). In contrast, NOX5 protein was not found in c-Abl immunoprecipitates from lysates of non-transfected HEK cells (Fig. 8C). Furthermore in the K562/NOX5 cells, the amount of NOX5 protein was considerably higher in cells that over-expressed the active GFP-c-Abl, as compared with GFP-KD-c-Abl-over-expressing cells (Fig. 8A, 8B). More importantly, the NOX5 content of the GFP-immunoprecipitates was increased by H_2O_2-treatment of K562/NOX5 cells over-expressing GFP-c-Abl (Fig. 8A, 8B).

Next we sought evidence for the presence of Abl and NOX5 proteins in the membrane fractions (Fig. 8D, 8E, 8F). NOX5, GFP-c-Abl and endogenous c-Abl were all detected in membranes of K562/NOX5 cells over-expressing GFP-c-Abl. H_2O_2 treatment increased the level of tagged GFP-c-Abl, as well as endogenous c-Abl, recovered in the membrane fractions. In cells over-expressing GFP-KD-c-Abl however, endogenous c-Abl was not detected in membrane fractions, although NOX5 was present. Furthermore, the level of GFP-KD-Abl was not significantly affected by H_2O_2 treatment.

NOX5 activity determined by the cytochrome c reduction assay was increased ~1.5-fold in membrane fractions prepared from K562/NOX5 cells that were pretreated with H_2O_2 as compared with cells incubated without H_2O_2 (Fig. 8G). An even greater effect of H_2O_2 pretreatment was observed in membranes isolated from K562/NOX5 cells expressing GFP-c-Abl (~2.5-fold increase), whereas no effect of H_2O_2 was observed in membranes isolated from K562/NOX5 cells expressing kinase dead GFP-c-Abl. In addition, higher basal activity was observed in membranes containing the over-expressed wild-type GFP-c-Abl (average superoxide production ~4 nmol/min/mg of protein). These results suggest that activated, membrane-associated c-Abl oligomers interact with NOX5 to enhance its activity.

Discussion

Here we report that H_2O_2 positively regulates NOX5 activity by c-Abl through a Ca^{2+}-mediated, redox-dependent signaling pathway and suggest a functional association between NOX5 and c-Abl. H_2O_2 stimulation of NOX5 was blocked by imatinib mesylate, an inhibitor of c-Abl tyrosine kinase, and by genistein, an inhibitor of Src tyrosine kinases, known activators of c-Abl [31,32]. However, in K562/NOX5 cells the over-expression of a constitutively active or inactive mutant of Src did not affect the regulation of NOX5 by H_2O_2, suggesting that Src

is not an upstream regulator of c-Abl. The effect of genistein might be the result of its unspecific action on other tyrosine kinases or c-Abl itself, since this inhibitor is known to be a broad tyrosine kinase inhibitor (Supplement Fig. 6). Although c-Abl can regulate the small GTPase Rac1 [33–35], we found that NOX5 activation by H_2O_2 was not mediated by this pathway (data not shown).

Imatinib mesylate inhibits Bcr-Abl, as well as c-Abl [26], both of which are expressed in K562 cells. In Bcr-Abl the N-terminal Bcr sequences are directly responsible for a constitutively active Abl tyrosine kinase [25]. Therefore, one might expect an effect of Bcr-Abl on the basal activity of NOX5 over-expressed in K562 cells. However, this was not the case. Our data suggest a more prominent role for c-Abl versus BCR-Abl, since in K562/NOX5 cells, over-expression of GFP-Abl increased basal superoxide-generating activity, but still allowed stimulation by H_2O_2 of ~3-fold. The smaller relative increase in NOX5 activity by H_2O_2 in these cells compared with K562/NOX5 cells that do not express GFP-c-Abl, may be due to saturation of the NOX5 system and/or to an enhanced level of activated c-Abl in the basal state. Indeed, the biochemical study shown in Fig. 7B demonstrates this latter point in that control cells (i.e. no H_2O_2) over-expressing c-Abl exhibited a very prominent band of activated c-Abl. Moreover, the extent of c-Abl activation in these cells by H_2O_2 exposure was about 2.7-fold, mirroring very closely the superoxide result shown in Fig. 4A. These results are consistent with studies showing that c-Abl is activated by H_2O_2 [29] and can induce an increase in ROS production when over-expressed in hematopoietic cells [3]. In contrast, the over-expression of KD-c-Abl abrogated the effect of H_2O_2. Furthermore, in the Bcr-Abl-negative HEK cells transiently transfected with either the GFP-c-Abl or GFP-KD-c-Abl protein, a similar effect of H_2O_2 was observed, although the relative stimulation of NOX5 activity by H_2O_2 in HEK cells was less pronounced than in K562 cells. This was perhaps due to differences in expression levels of NOX5 and/or antioxidant protein expression levels (e.g. catalase, SOD, peroxiredoxin, glutathione peroxidase), thereby affecting the H_2O_2 amplification loop potential. In accord with this hypothesis, an immunoblot experiment performed on whole cell lysates showed a lower level of NOX5 and a higher level of catalase in HEK/NOX5 cells compared with K562/NOX5 cells (data not shown). Collectively, these results demonstrate that c-Abl protein is a required intermediate for H_2O_2 stimulation of NOX5 NADPH oxidase.

Our confocal imaging studies provide spatial and temporal data on the events leading to superoxide formation in response to H_2O_2. Red fluorescence corresponding to superoxide production was observed near the plasma membrane, as well as in cytoplasmic vesicles. The fact that SOD abrogated the red fluorescence throughout the cell suggests that the initial events in this pathway most likely occur at the plasma membrane. These observations are consistent with the data obtained with the Diogenes reagent using whole cells, since only extracellular superoxide is detected with this assay. The fact that we did not detect red fluorescence outside the cell near the plasma membrane is probably due to rapid diffusion and subsequent dilution of superoxide in the medium. These results suggest that vesicular trafficking allows plasma membrane components to network within the cell. In accordance with this suggestion, previous reports show the presence of NOX5 protein at both the plasma membrane and the endoplasmic reticulum [36,37]. Furthermore, similar to our results showing compartmentalization of superoxide, Li and colleagues demonstrated that superoxide produced by NOX2 was generated in endosomes [16].

Since NOX5 is activated by the binding of Ca^{2+} to its N-terminal EF hand domains, we investigated whether Ca^{2+} was required for NOX5 activation by H_2O_2. Studies with the Ca2 + chelator BAPTA showed that H_2O_2 stimulated an influx of Ca^{2+} from the extracellular medium, and this, rather than release of intracellular Ca^{2+} stores, was responsible for NOX5 activation Interestingly, DPI and SOD reduced Ca^{2+} entry induced by H_2O_2, indicating a role for superoxide generation in H_2O_2 signaling. Kinetic studies suggested that the initial phase

of Ca^{2+} influx was mediated predominantly by exogenous H_2O_2, whereas the subsequent phase required superoxide generated by early NOX5 activity. Regulation of Ca^{2+} influx by ROS has been previously observed [38–40]. However, whether the Ca^{2+} influx is the result of a reaction product of superoxide and hydrogen peroxide (e.g. hydroxyl radical) or if these individual ROS molecules are each able to induce Ca^{2+} influx is an interesting question that remains to be answered.

Using both confocal microscopy and the chemiluminescence superoxide assay, we also showed that ionomycin induced NOX5-dependent superoxide production equally well in cells whether they expressed wild-type or kinase-dead c-Abl, whereas active c-Abl was required for H_2O_2 stimulation (Fig. 6B, 6C and Supplement Fig. 7). A significant difference between H_2O_2 and ionomycin may well be the magnitude of Ca^{2+} influx induced, although spatial and kinetic features of cytosolic Ca^{2+} changes may also differ between the two stimuli. NOX5 protein exhibits a lower affinity for calcium [13] than do other calcium-regulated proteins, such as calmodulin and Ca^{2+}-ATPase [41, 42]. Therefore the calcium influx induced by 100μM H_2O_2 appears to be insufficient by itself to activate NOX5. Thus, activated c-Abl may be required to enhance the sensitivity of NOX5 to calcium. This mechanism is reminiscent of a recent report showing that the phosphorylation of NOX5 induced by phorbol esters can facilitate enzyme activation in the presence of sub-optimal levels of intracellular calcium [37]. Whether NOX5 activity is regulated via its phosphorylation by c-Abl remains to be determined and is currently under investigation in our laboratory.

The confocal images showed that GFP-tagged Abl was mainly localized to the cytosol. Upon H_2O_2 treatment, wild-type c-Abl, but not kinase-dead c-Abl, co-localized with sites of superoxide production. These events were dependent on the tyrosine kinase activity of c-Abl, as well as on Ca^{2+} influx. Immunoprecipitation studies showed that mainly wild-type GFP-c-Abl formed oligomers with endogenous c-Abl, but not with Bcr-Abl. Furthermore, endogenous membrane-associated c-Abl was detected only in cells expressing the wild-type GFP-c-Abl. Interestingly, wild-type c-Abl possesses the proper N-terminal domain for myristoylation, which allows the protein to become anchored in cell membranes [43]. In addition, previous reports indicate that over-expression of tagged and untagged c-Abl induces c-Abl oligomerization in a kinase-dependent manner that requires the N-terminal region [30]. These results support an important role for endogenous c-Abl since this is the only form that allows the presence of tagged wild-type c-Abl in the membrane where NOX5 is located. Although we occasionally observed low levels of GFP-KD-c-Abl in the membranes, this was not associated with endogenous c-Abl and likely resulted from nonspecific interaction due to over-expression.

Collectively, these results support the concept that exposure to H_2O_2 leads to a sequence of events that includes c-Abl protein tyrosine phosphorylation, oligomerization, and Ca^{2+}-dependent translocation, resulting in the membrane co-localization of activated c-Abl and NOX5 proteins (see signaling model shown in Fig. 9). Since BAPTA can cause direct inhibition of NOX5 and block c-Abl relocalization, we cannot be certain that c-Abl relocalization is essential for NOX5 activation. On the other hand, the coimmunoprecipitation of GFP-c-Abl and NOX5 indicates a close interaction between the two proteins and points to the potential importance of cAbl translocation. In addition, data from a broken cell system support the notion of functional interaction between Abl and NOX5 proteins, since increased NOX5 activity correlated with increased c-Abl content in membrane preparations.

Our data demonstrate for the first time that NOX5 is regulated by c-Abl in a redox-dependent manner and suggest a functional association between NOX5 and c-Abl. Although the model proposed in Figure 9 describes an autocrine mechanism of amplification of H_2O_2 signaling, the diffusible character of H_2O_2 supports, in addition, paracrine regulation of adjacent NOX-expressing cells. Ubiquitously expressed, c-Abl has been shown to play a role in cell cycle

regulation and in cellular responses to growth factor signaling, oxidative stress, and DNA damage [44] and previous studies suggest that c-Abl functions are specified in part by its subcellular localization. We propose that c-Abl located in the membrane plays an important role in redox signaling. Since NOX5 is highly expressed in testis and in lymphoid tissues, there are potential roles for H_2O_2-NOX5 regulation in their Ca2+-activated, redox-dependent processes such as sperm-oocyte fusion, cell proliferation, and cytokine secretion [45–47]. NOX5 has also been reported in human endothelial cells where it may play a role in ROS-dependent vascular physiology and pathophysiology [36].

Supplementary Material

Refer to Web version on PubMed Central for supplementary material.

Acknowledgements

This work was supported by Grants AI020866, AG019519 and AI034879 from the National Institutes of Health. The confocal microscopy studies were performed in the Institutional Optical Imaging Facility of the University of Texas Health Science Center at San Antonio, which is supported by NIH grants P30-CA054174 (San Antonio Cancer Institute), P30-AG013319 (Nathan Shock Center), and P01-AG019316 (Aging, Oxidative Stress and Cell Death). The authors would like to thank Hanna Abboud and Alain Virion for helpful discussions and critical reviews of the manuscript, John Cornell for insightful advice on statistical analysis, and Victoria Frohlich for expert guidance on the confocal microscope image acquisition and analysis.

Abbreviations The abbreviations used are

BAPTA
: 1,2-bis(2-aminophenoxy) ethane-*N*,*N*,*N*,*N*-tetraacetic acid

DPI
: diphenylene iodonium

EDTA
: ethylenediaminetetraacetic acid

FAD
: flavin adenine dinucleotide

GFP
: green fluorescent protein

HE
: hydroethidine

HEK
: human embryonic kidney

H_2O_2
: hydrogen peroxide

NADPH
: nicotinamide adenine dinucleotide phosphate reduced

NOX
: NADPH oxidase

NOX5
: NADPH oxidase NOX5

PBS
phosphate-buffered saline

PBS-G
PBS containing 10 mM glucose

PVDF
polyvinylidene fluoride

ROS
reactive oxygen species

SERCA
sarco-endoplasmic reticulum Ca^{2+}-ATPase

SOD
superoxide dismutase

References

1. Bae YS, Kang SW, Seo MS, Baines IC, Tekle E, Chock PB, Rhee SG. Epidermal Growth Factor (EGF)-induced Generation of Hydrogen Peroxide. Role in EGF receptor-mediated tyrosine phosphorylation. J Biol Chem 1997;272:217–221. [PubMed: 8995250]
2. Lo YYC, Cruz TF. Involvement of Reactive Oxygen Species in Cytokine and Growth Factor Induction of c-fos Expression in Chondrocytes. J Biol Chem 1995;270:11727–11730. [PubMed: 7744816]
3. Sattler M, Verma S, Shrikhande G, Byrne CH, Pride YB, Winkler T, Greenfield EA, Salgia R, Griffin JD. The BCR/ABL Tyrosine Kinase Induces Production of Reactive Oxygen Species in Hematopoietic Cells. J Biol Chem 2000;275:24273–24278. [PubMed: 10833515]
4. Sattler M, Winkler T, Verma S, Byrne CH, Shrikhande G, Salgia R, Griffin JD. Hematopoietic Growth Factors Signal Through the Formation of Reactive Oxygen Species. Blood 1999;93:2928–2935. [PubMed: 10216087]
5. Sundaresan M, Yu ZX, Ferrans VJ, Irani K, Finkel T. Requirement for generation of H_2O_2 for platelet-derived growth factor signal transduction. Science 1995;270:296–299. [PubMed: 7569979]
6. Chen Q, Olashaw N, Wu J. Participation of reactive oxygen species in the lysophosphatidic acid-stimulated mitogen-activated protein kinase kinase activation pathway. J Biol Chem 1995;270:28499–28502. [PubMed: 7499358]
7. Zafari AM, Ushio-Fukai M, Akers M, Yin Q, Shah A, Harrison DG, Taylor WR, Griendling KK. Role of NADH/NADPH oxidase-derived H_2O_2 in Angiotensin II–induced vascular hypertrophy. Hypertension 1998;32:488–495. [PubMed: 9740615]
8. Park HS. Cutting edge: direct interaction of TLR4 with NAD(P)H oxidase 4 isozyme is essential for lipopolysaccharide-induced production of reactive oxygen species and activation of NF-kappa B. The Journal of Immunology 2004;173:3589–93. [PubMed: 15356101]
9. Bedard K, Krause K-H. The NOX Family of ROS-generating NADPH oxidases: physiology and pathophysiology. Physiol Rev 2007;87:245–313. [PubMed: 17237347]
10. Nauseef WM. Assembly of the phagocyte NADPH oxidase. Histochemistry and Cell Biology 2004;V122:277–291. [PubMed: 15293055]
11. Quinn MT, Gauss KA. Structure and regulation of the neutrophil respiratory burst oxidase: comparison with nonphagocyte oxidases. J Leukoc Biol 2004;76:760–781. [PubMed: 15240752]
12. Banfi B, Molnar G, Maturana A, Steger K, Hegedus B, Demaurex N, Krause K-H. A Ca^{2+}-activated NADPH oxidase in Testis, Spleen, and Lymph Nodes. J Biol Chem 2001;276:37594–37601. [PubMed: 11483596]
13. Banfi B, Tirone F, Durussel I, Knisz J, Moskwa P, Molnar GZ, Krause K-H, Cox JA. Mechanism of Ca^{2+} Activation of the NADPH oxidase 5 (NOX5). J Biol Chem 2004;279:18583–18591. [PubMed: 14982937]

14. Stone JR, Yang S. Hydrogen peroxide: A signaling messenger. Antioxid Redox Signal 2006;8:243–270. [PubMed: 16677071]
15. Touyz RM. Reactive oxygen species as mediators of calcium signaling by angiotensin II: Implications in vascular physiology and pathophysiology. Antioxid Redox Signal 2005;7:1302–1314. [PubMed: 16115036]
16. Li Q, Harraz MM, Zhou W, Zhang LN, Ding W, Zhang Y, Eggleston T, Yeaman C, Banfi B, Engelhardt JF. Nox2 and Rac1 Regulate H_2O_2-dependent recruitment of TRAF6 to endosomal interleukin-1 receptor complexes. Mol Cell Biol 2006;26:140–154. [PubMed: 16354686]
17. Clark RA, Valente AJ. Nuclear factor kappa B activation by NADPH oxidases. Mechanisms of Ageing and Development Hormone receptors, genes, ageing and Arun Roy: A tribute to Professor Arun K. Roy 2004;125:799–810.
18. Tsai KKC, Yuan ZM. c-Abl stabilizes p73 by a phosphorylation-augmented interaction. Cancer Res 2003;63:3418–3424. [PubMed: 12810679]
19. Schaffner W, Weissman C. A rapid, sensitive, and specific method for the determination of protein in dilute solution. Anal Biochem 1973;56:502–514. [PubMed: 4128882]
20. Massey V. The microestimation of succinate and the extinction coefficient of cytochrome c. Biochem Biophys Acta 1959;34:255–256. [PubMed: 14422133]
21. Borregaard N, Heiple J, Simons E, Clark R. Subcellular localization of the b-cytochrome component of the human neutrophil microbicidal oxidase: translocation during activation. J Cell Biol 1983;97:52–61. [PubMed: 6408102]
22. Sbarra AJ, Karnovsky ML. The biochemical basis of phagocytosis. Metabolic changes during the ingestion of particles by polymorphonuclear leukocytes. J Biol Chem 1959;234:1355–1362. [PubMed: 13654378]
23. El Jamali A, Freund C, Rechner C, Scheidereit C, Dietz R, Bergmann MW. Reoxygenation after severe hypoxia induces cardiomyocyte hypertrophy in vitro: activation of CREB downstream of GSK3β. FASEB J 2004:03-1054fje.
24. Touyz RM, Schiffrin EL. Reactive oxygen species in vascular biology: implications in hypertension. Histochem Cell Biol 2004;V122:339–352. [PubMed: 15338229]
25. Muller AJ, Young JC, Pendergast AM, Pondel M, Landau NR, Littman DR, Witte ON. BCR first exon sequences specifically activate the BCR/ABL tyrosine kinase oncogene of Philadelphia chromosome-positive human leukemias. Mol Cell Biol 1991;11:1785–1792. [PubMed: 2005881]
26. Druker BJ, Tamura S, Buchdunger E, Ohno S, Segal GM, Fanning S, Zimmermann J, Lydon NB. Effects of a selective inhibitor of the Abl tyrosine kinase on the growth of Bcr-Abl positive cells. Nat Med 1996;2:561–566. [PubMed: 8616716]
27. Blatter LA, Wier WG. Intracellular diffusion, binding, and compartmentalization of the fluorescent calcium indicators indo-1 and fura-2. Biophys J 1990;58:1491–1499. [PubMed: 2275965]
28. Brasher BB, Van Etten RA. c-Abl has high intrinsic tyrosine kinase activity that is stimulated by mutation of the Src Homology 3 domain and by autophosphorylation at two distinct regulatory tyrosines. J Biol Chem 2000;275:35631–35637. [PubMed: 10964922]
29. Kumar S, Mishra N, Raina D, Saxena S, Kufe D. Abrogation of the cell death response to oxidative stress by the c-Abl tyrosine kinase Inhibitor STI571. Mol Pharmacol 2003;63:276–282. [PubMed: 12527798]
30. Fan P-D, Cong F, Goff SP. Homo- and hetero-oligomerization of the c-Abl kinase and Abelson-interactor-1. Cancer Res 2003;63:873–877. [PubMed: 12591740]
31. Furstoss O, Dorey K, Simon V, Barila D, Superti-Furga G, Roche S. c-Abl is an effector of Src for growth factor-induced c-myc expression and DNA synthesis. EMBO J 2002;21:514–524. [PubMed: 11847100]
32. Plattner R, Kadlec L, DeMali KA, Kazlauskas A, Pendergast AM. c-Abl is activated by growth factors and Src family kinases and has a role in the cellular response to PDGF. Genes Dev 1999;13:2400–2411. [PubMed: 10500097]
33. Boureux A, Furstoss O, Simon V, Roche S. Abl tyrosine kinase regulates a Rac/JNK and a Rac/Nox pathway for DNA synthesis and Myc expression induced by growth factors. J Cell Sci 2005;118:3717–3726. [PubMed: 16076903]

34. Mizuchi D, Kurosu T, Kida A, Jin Z-H, Jin A, Arai A, Miura O. BCR/ABL activates Rap1 and B-Raf to stimulate the MEK/Erk signaling pathway in hematopoietic cells. Biochem Biophys Res Com 2005;326:645–651. [PubMed: 15596148]
35. Skorski T, Wlodarski P, Daheron L, Salomoni P, Nieborowska-Skorska M, Majewski M, Wasik M, Calabretta B. BCR/ABL-mediated leukemogenesis requires the activity of the small GTP-binding protein Rac. PNAS 1998;95:11858–11862. [PubMed: 9751755]
36. BelAiba RS, Djordjevic T, Petry A, Diemer K, Bonello S, Banfi B, Hess J, Pogrebniak A, Bickel C, Gorlach A. NOX5 variants are functionally active in endothelial cells. Free Radic Biol Med 2007;42:446–459. [PubMed: 17275676]
37. Jagnandan D, Church JE, Banfi B, Stuehr DJ, Marrero MB, Fulton DJR. Novel mechanism of activation of NADPH oxidase 5 (NOX5): Calcium-sensitization via phosphorylation. J Biol Chem 2006;282:6494–6507. [PubMed: 17164239]
38. Burlando B, Viarengo A. Ca^{2+} is mobilized by hydroxyl radical but not by superoxide in RTH-149 cells: The oxidative switching-on of Ca^{2+} signaling. Cell Calcium 2005;38:507–513. [PubMed: 16140374]
39. Hu Q, Corda S, Zweier JL, Capogrossi MC, Ziegelstein RC. Hydrogen peroxide induces intracellular calcium oscillations in human aortic endothelial cells. Circulation 1998;97:268–275. [PubMed: 9462529]
40. Lounsbury KM, Hu Q, Ziegelstein RC. Calcium signaling and oxidant stress in the vasculature. Free Radic Biol Med 2000;28:1362–1369. [PubMed: 10924855]
41. Shifman JM, Choi MH, Mihalas S, Mayo SL, Kennedy MB. Ca^{2+}/calmodulin-dependent protein kinase II (CaMKII) is activated by calmodulin with two bound calciums. PNAS 2006;103:13968–13973. [PubMed: 16966599]
42. Waggoner JR, Huffman J, Froehlich JP, Mahaney JE. Phospholamban inhibits Ca^{2+}-ATPase conformational changes involving the E2 intermediate. Biochemistry 2007;46:1999–2009. [PubMed: 17261028]
43. Hantschel O, Nagar B, Guettler S, Kretzschmar J, Dorey K, Kuriyan J, Superti-Furga GA. Myristoyl/Phosphotyrosine switch regulates c-Abl. Cell 2003;112:845–857. [PubMed: 12654250]
44. Van Etten RA. Cycling, stressed-out and nervous: cellular functions of c-Abl. Trends Cell Biol 1999;9:179–186. [PubMed: 10322452]
45. Ginn-Pease ME, Whisler RL. Redox signals and NF-[kappa]B activation in T cells. Free Radl Biol Med 1998;25:346–361.
46. Kaisho T, Takeda K, Tsujimura T, Kawai T, Nomura F, Terada N, Akira S. IκBα is essential for mature B cell development and function. J Exp Med 2001;193:417–426. [PubMed: 11181694]
47. Schreck RRP, Baeuerle PA. Reactive oxygen intermediates as apparently widely used messengers in the activation of the NF-kappa B transcription factor and HIV-1. EMBO J 1991;10:2247–2258. [PubMed: 2065663]

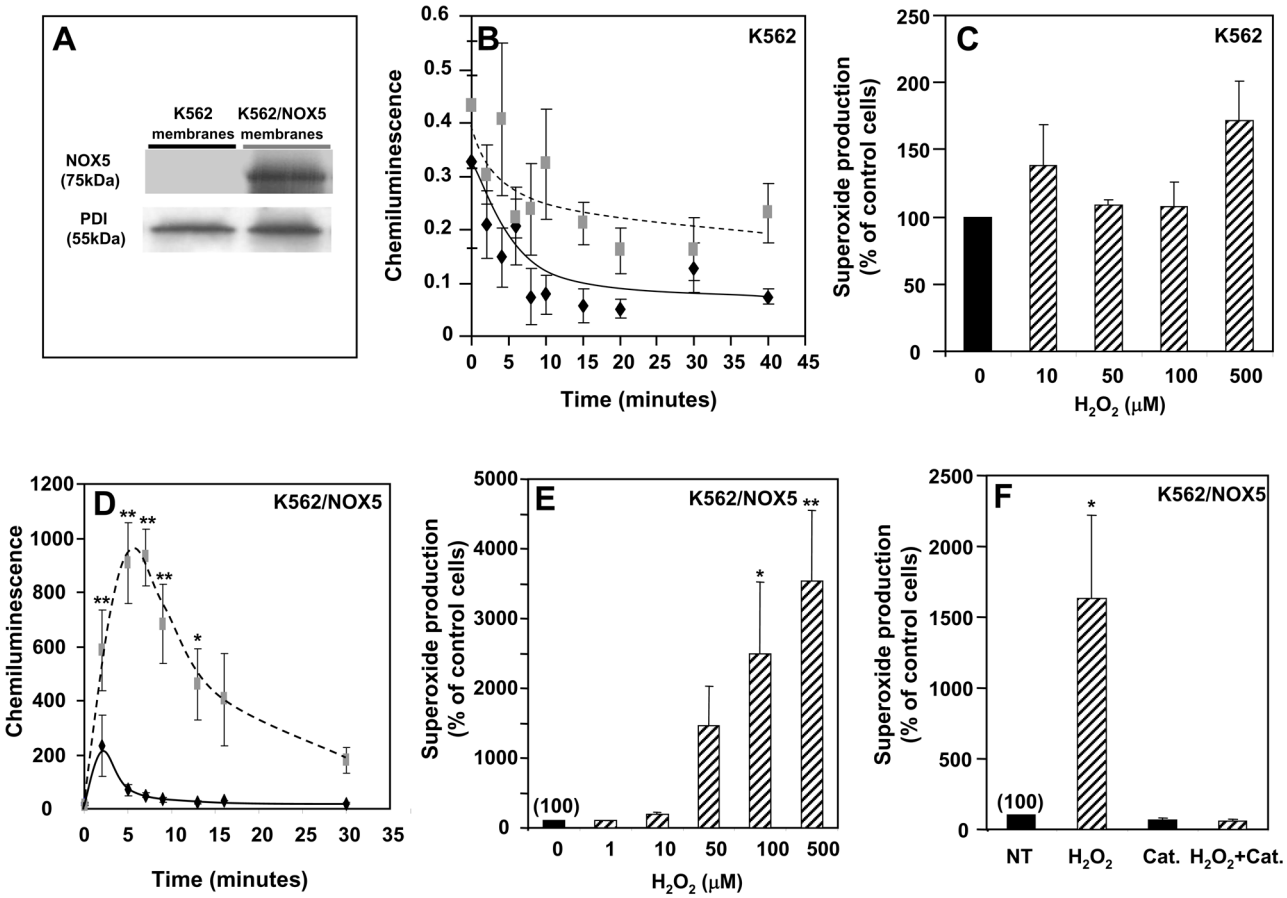

Fig. 1. Dose- and time-dependent effect of H_2O_2 on superoxide production in K562 cells and K562/NOX5 cells

K562 and K562/NOX5 cells were assayed for superoxide production using the Diogenes reagent and for NOX5 protein by immunoblot. (A) Immunoblot of crude membranes using antibodies to NOX5 and protein disulfide isomerase (PDI; loading control). (B, D) Chemiluminescence from cells incubated with (broken line) or without (solid line) 100 μM H_2O_2 for the indicated times. (C, E) Superoxide production was measured in cells incubated for 10 minutes with various concentrations of H_2O_2 (0–500 μM). After normalization by subtraction of the zero-time value of the chemiluminescence output, the area under the curve was calculated as a measure of total superoxide production. (F) Superoxide production was determined in whole K562/NOX5 cells incubated with or without 100 μM H_2O_2 and/or catalase (900 U). After normalization as above, the superoxide production was expressed as a percent of non-treated cells without H_2O_2 (NT). The data expressed are the means +/− SEM of 3 to 6 independent experiments. Asterisks indicate statistical significance versus control cells without H_2O_2: * $P<0.05$, ** $P<0.01$.

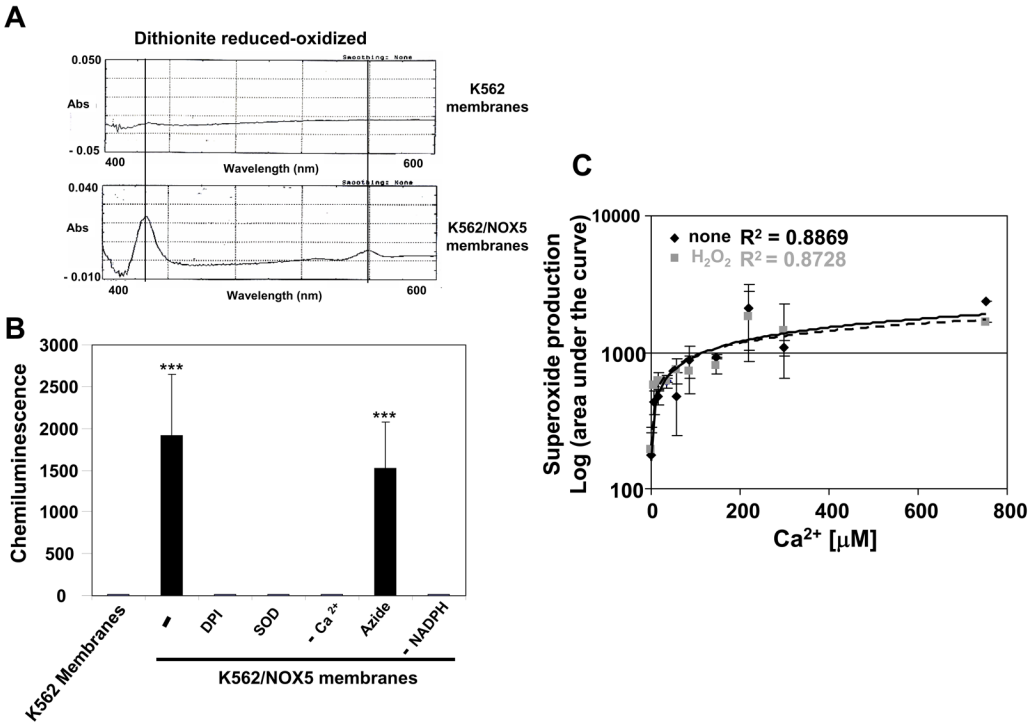

Fig. 2. Effect of H_2O_2 on cell-free NOX5 activity

(A) Difference spectra of dithionite-reduced minus oxidized samples of crude membranes from K562 and K562/NOX5 cells (B) Superoxide production in crude membrane preparations. The assay was performed as described in Experimental Procedure using the Diogenes reagent in the presence of SOD (400 U/ml), DPI (10 μM), or sodium azide (1 mM), or in the absence of NADPH (−) or Ca^{2+} (−), as indicated. After normalization by subtraction of the zero-time value of the chemiluminescence output, the area under the curve was calculated as a measure of total superoxide production. *** $P < 0.001$ = statistical significance versus control K562 membranes. (C) Superoxide produced by K562/NOX5 membranes was determined in the presence of 100 μM H_2O_2 and increasing free Ca2+ concentrations. The values obtained are expressed as in B. No significant difference was observed versus the value obtained in the absence of H_2O_2. The data shown are the means +/− SEM of 3 to 7 independent experiments.

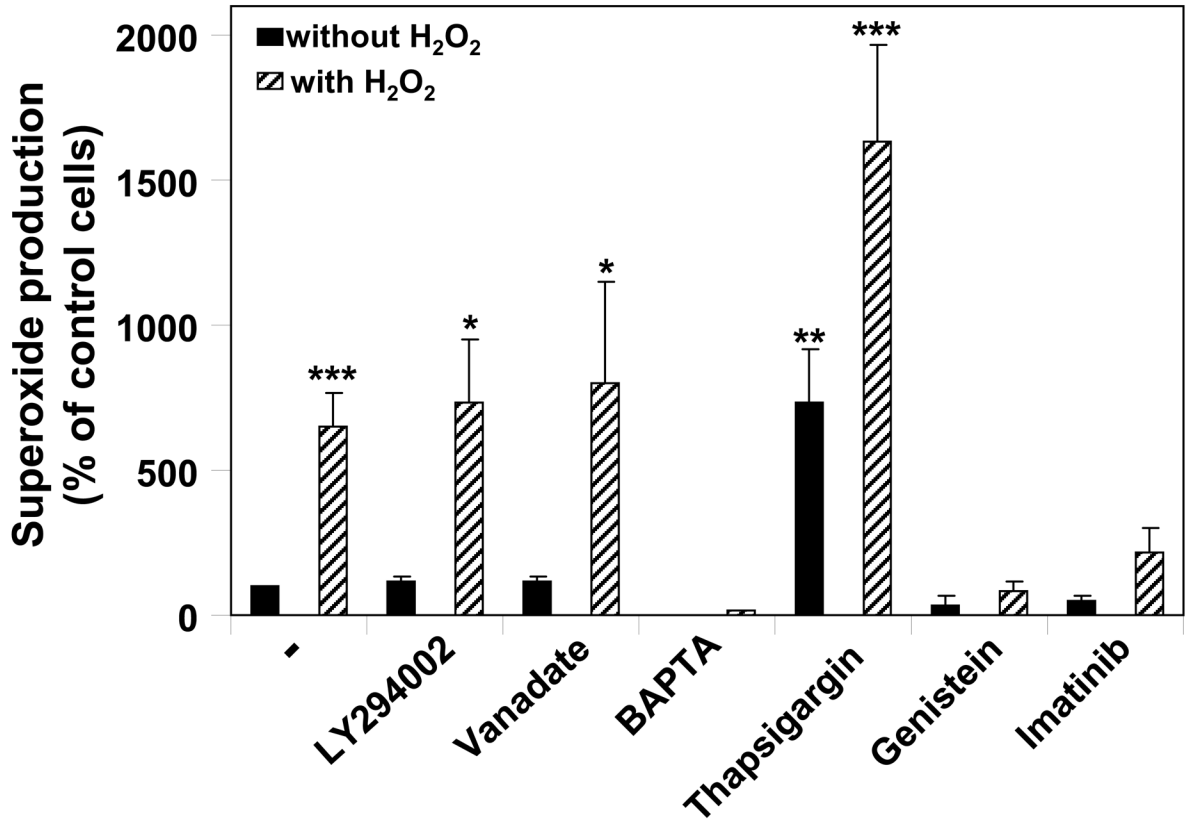

Fig. 3. Effect of various inhibitors on H_2O_2-NOX5 regulation

K562/NOX5 cells were pretreated with the indicated inhibitors, as described in Experimental Procedures. The cells were then tested for superoxide production in the presence or absence of H_2O_2 100 μM for 10 minutes. Superoxide production was expressed as a percent of the value obtained for non-pretreated cells in the absence of H_2O_2. The data are the means +/− SEM of 5 to 10 independent experiments. Asterisks indicate statistical significance versus control cells without H_2O_2. * $P < 0.05$; ** <0.01.

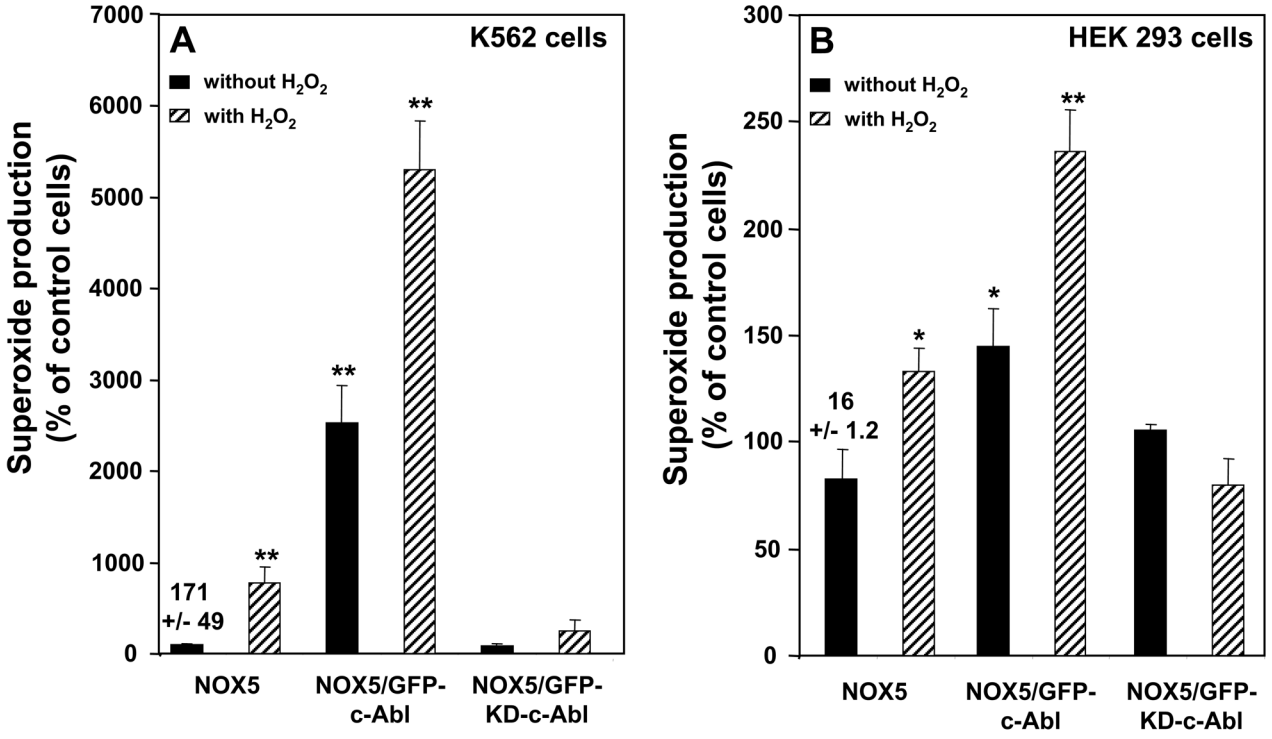

Fig. 4. Effect of GFP-tagged wild-type and kinase-dead c-Abl on H_2O_2-NOX5 regulation

Superoxide production was determined in the presence or absence of 100 μM H_2O_2. (A) K562 cells stably expressing GFP-c-Abl or GFP-KD-c-Abl were transfected with the pRep4 vector encoding the NOX5 protein. (B) HEK/NOX5 cells transiently transfected with either an empty vector or the wild-type c-Abl or kinase-dead c-Abl. Superoxide production was expressed as a percent of the value obtained for non-treated cells in the absence of H_2O_2. The data are the means +/− SEM of 3 to 4 independent experiments. Asterisks indicate statistical significance versus control cells without H_2O_2 * $P < 0.05$; ** $P < 0.01$, Numbers above the first column of each graph represent the mean +/− SEM of the chemiluminescence output observed in those samples at 10 minutes.

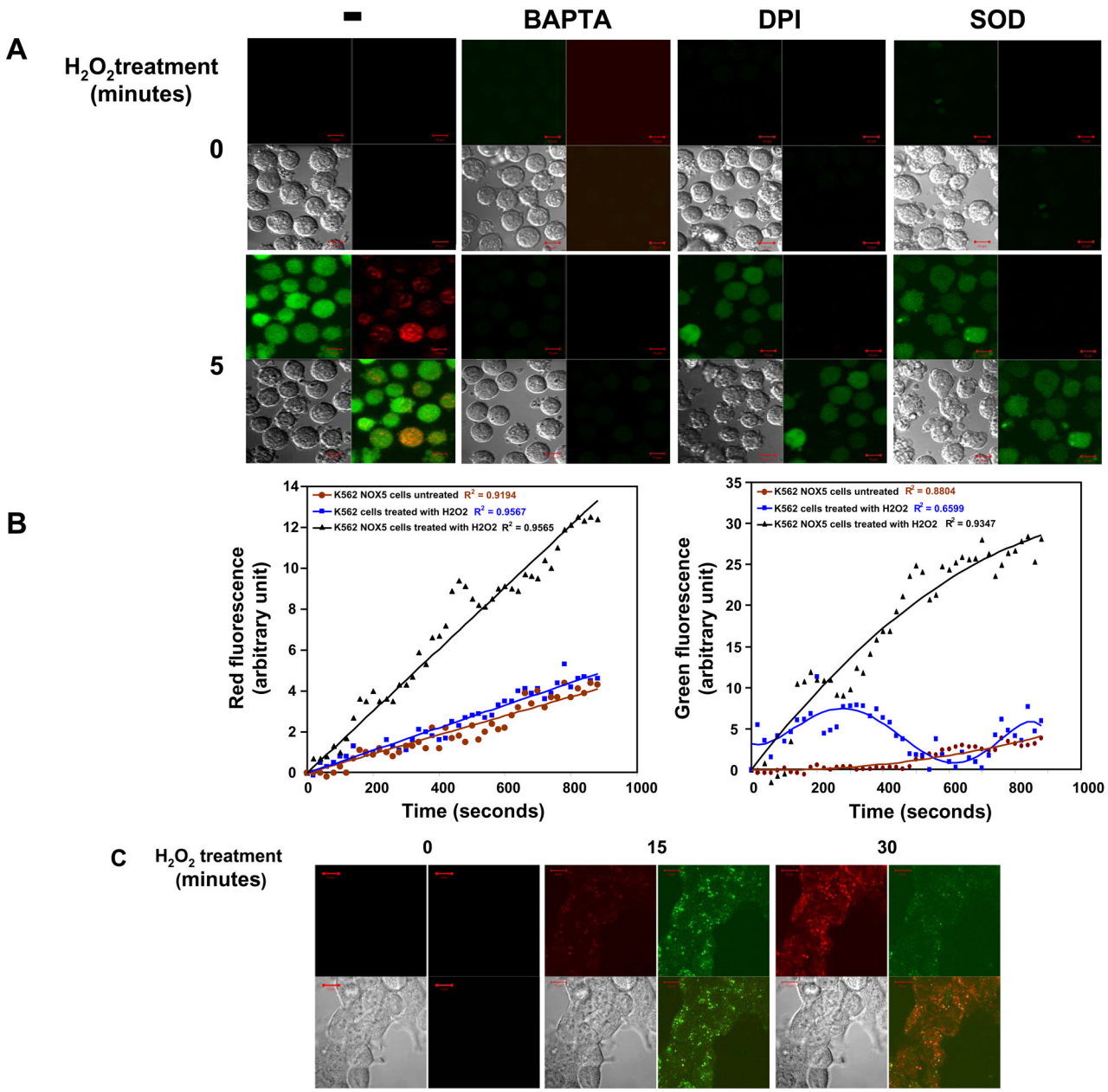

Fig. 5. Confocal microscopy of H_2O_2-induced superoxide and calcium influx in K562/NOX5 and HEK/NOX5 cells

(A) K562/NOX5 cells were loaded with fluo-4 (green fluorescence, calcium influx) and HE (red fluorescence, superoxide production), then stimulated with 100 μM H_2O_2. The effects of BAPTA (50 μM), DPI (50 μM), or SOD (400 U/ml) on NOX5 regulation by H_2O_2 were analyzed. Confocal images using a Zeiss microscope were recorded for up to 30 minutes using dual excitation 488/543nm. Images from the 0 and 5 minute time points are shown. Each set of four photomicrograph panels correspond to calcium influx (green fluorescence – top left), superoxide production (red fluorescence - top right),, the differential interference contrast (DIC) image (bottom left), and a merge picture of the fluorescent images (bottom right). The scale bar indicates a size of 10μm. (B) The fluorescence intensity levels from a representative experiment are shown using either K562/NOX5 cells (black line) or K562 cells treated with

H_2O_2 (blue line). Fluorescence levels in K562/NOX5 cells in the absence of H_2O_2 were also analyzed (brown line). After normalization by subtraction of the zero-time value, fluorescence was plotted as the mean for a field of approximately 15 cells. For each data set, curve-fitting analysis was carried using Excel and the best curve fit shown together with the coefficient of correlation. (C) HEK/NOX5 cells were loaded with fluo-4 and HE and confocal imaging carried out as in (A) using a single excitation wavelength (488nm).

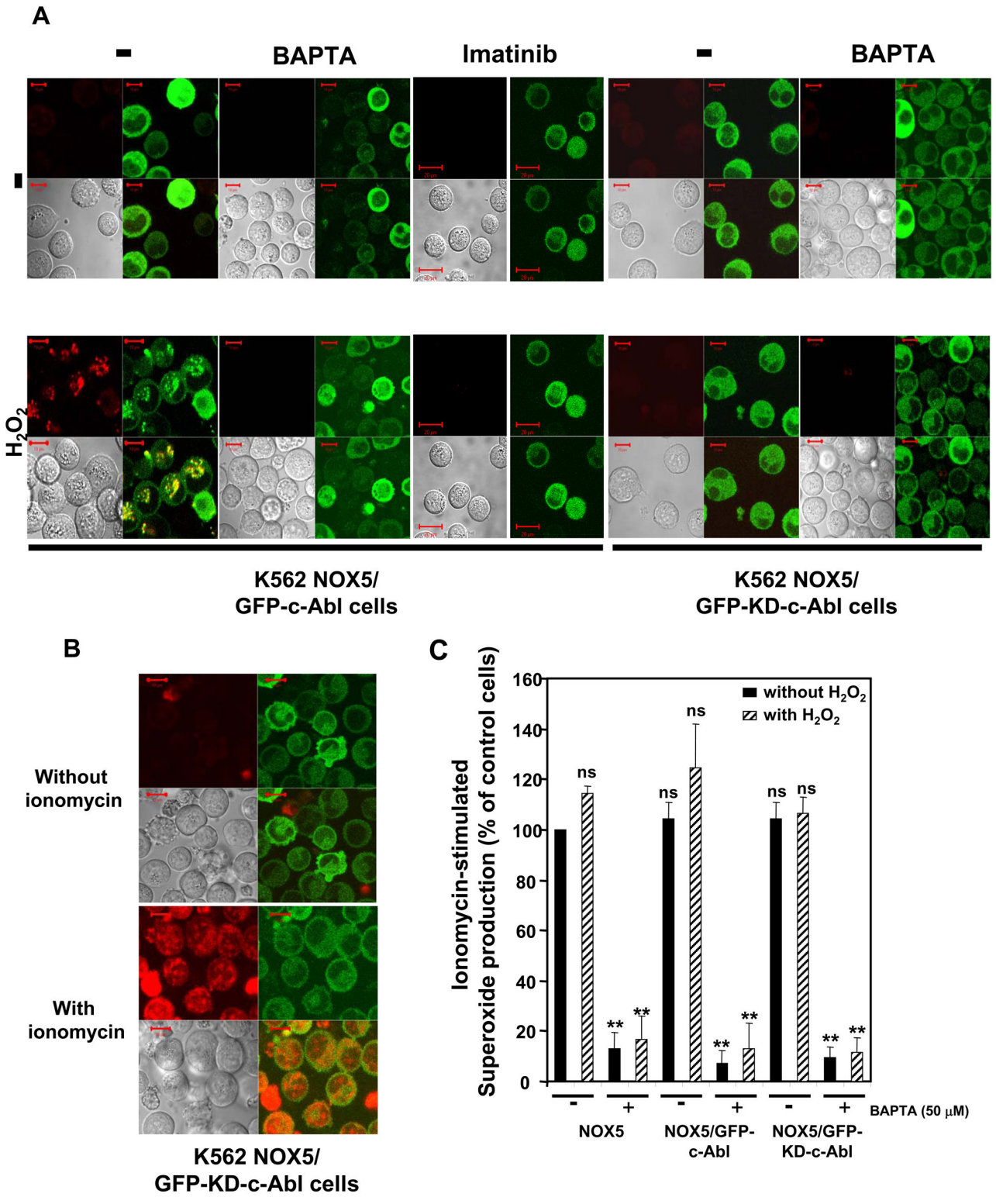

Fig. 6. Role of calcium in c-Abl-dependent induction of NOX5 by H_2O_2

(A) K562/NOX5 cells expressing either wild-type or kinase-dead GFP-c-Abl (green fluorescence) were loaded with HE (red fluorescence) and stimulated or not with 100 μM

H_2O_2 in the presence or absence of BAPTA (50 μM), or pretreated with imatinib as described in Experimental Procedures. (B) K562/NOX5 cells expressing the kinase-dead GFP-c-Abl (green fluorescence) were loaded with HE and stimulated with ionomycin (100 nM). Confocal images were recorded using a Zeiss microscope as described in Fig. 5. The scale bar indicates a size of 10 μm. (C) Superoxide assays were performed in K562/NOX5 cells and in K562/NOX5 cells expressing either wild-type c-Abl or kinase-dead c-Abl. The cells were all stimulated with ionomycin (100 nM) after a pre-incubation of 10 minutes with or without H_2O_2 in the presence or absence of BAPTA. Superoxide production was expressed as a percent of the value obtained for non-treated cells in the absence of H_2O_2. The data are the means +/− SEM of 3 to 5 independent experiments. Asterisks indicate statistical significance versus control cells without H_2O_2. ** $P < 0.01$ or ns.

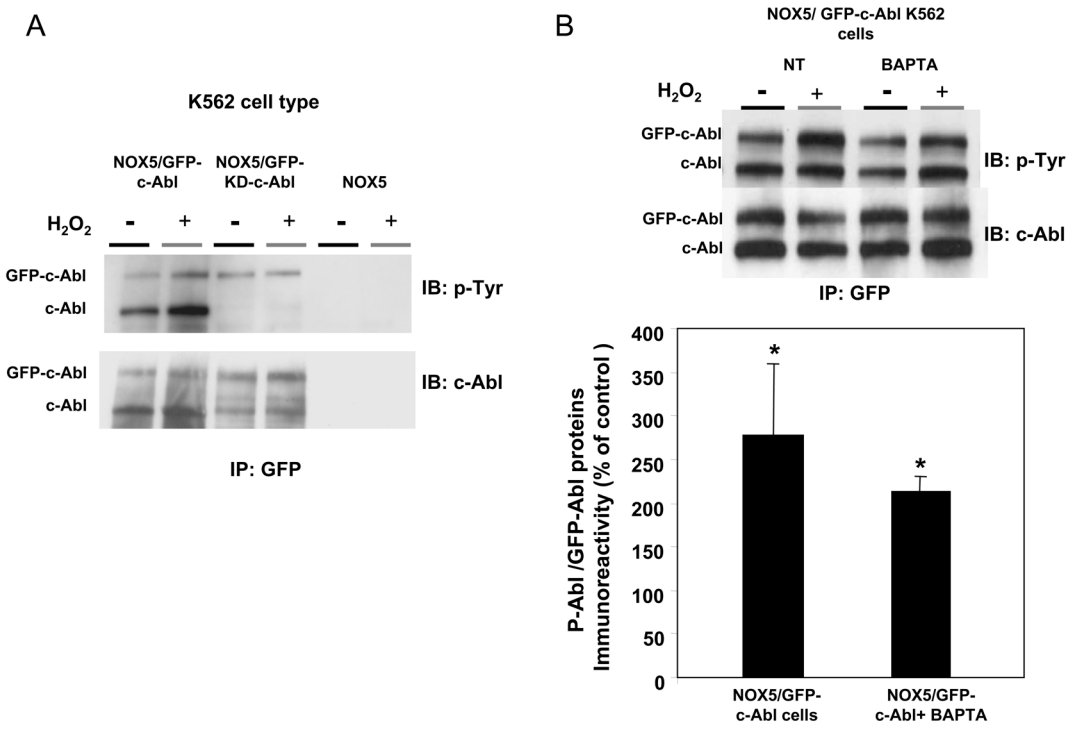

Fig. 7. Effect of H_2O_2 on c-Abl phosphorylation

(A) Immunoprecipitation of GFP-tagged Abl was performed using anti-GFP antibodies and 250 μg of proteins obtained from lysates of K562/NOX5 cell expressing either kinase-active GFP-c-Abl or the kinase-dead GFP-c-Abl. The immunoprecipitated proteins were immunoblotted with phosphotyrosine or c-Abl antibody. K562/NOX5 cells were used as a negative control. (B) Immunoprecipitation experiment were performed as in A, except that the K562/NOX5 cells expressing wild-type GFP-c-Abl were either untreated or incubated with BAPTA (50 μM) and then treated (or not treated) with 100 μM H_2O_2 for 10 minutes. In the GFP immunoprecipitates, the levels of phosphorylated Abl proteins (GFP-c-Abl plus endogenous c-Abl) were calculated from their individual autoradiographic densities and normalized to the corresponding GFP-tagged protein level. All values obtained were then expressed as a percentage of the control value obtained from H_2O_2-untreated cells. Data are the mean +/− SEM of 3 independent experiments. Asterisks indicate statistical significance versus cells without H_2O_2. * P <0.05, ** P <0.01.

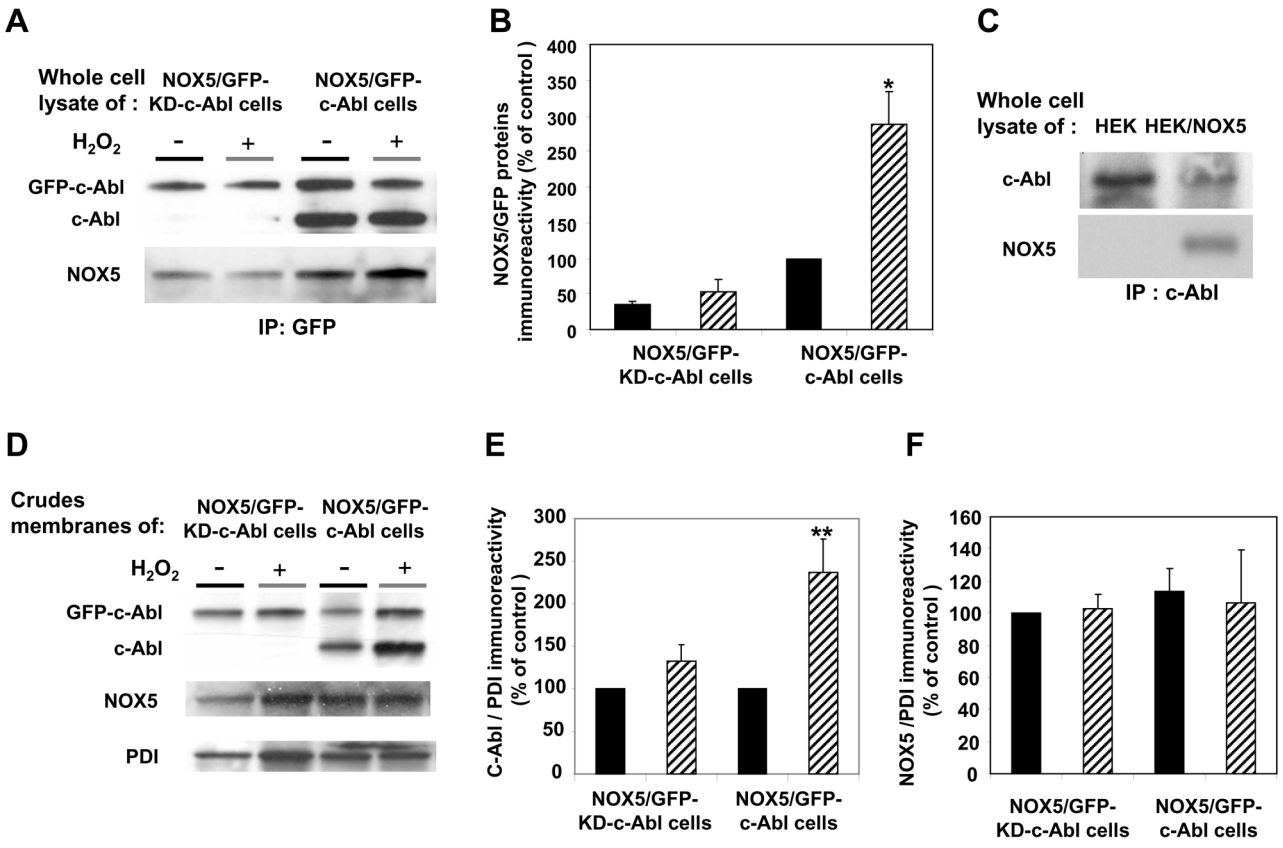

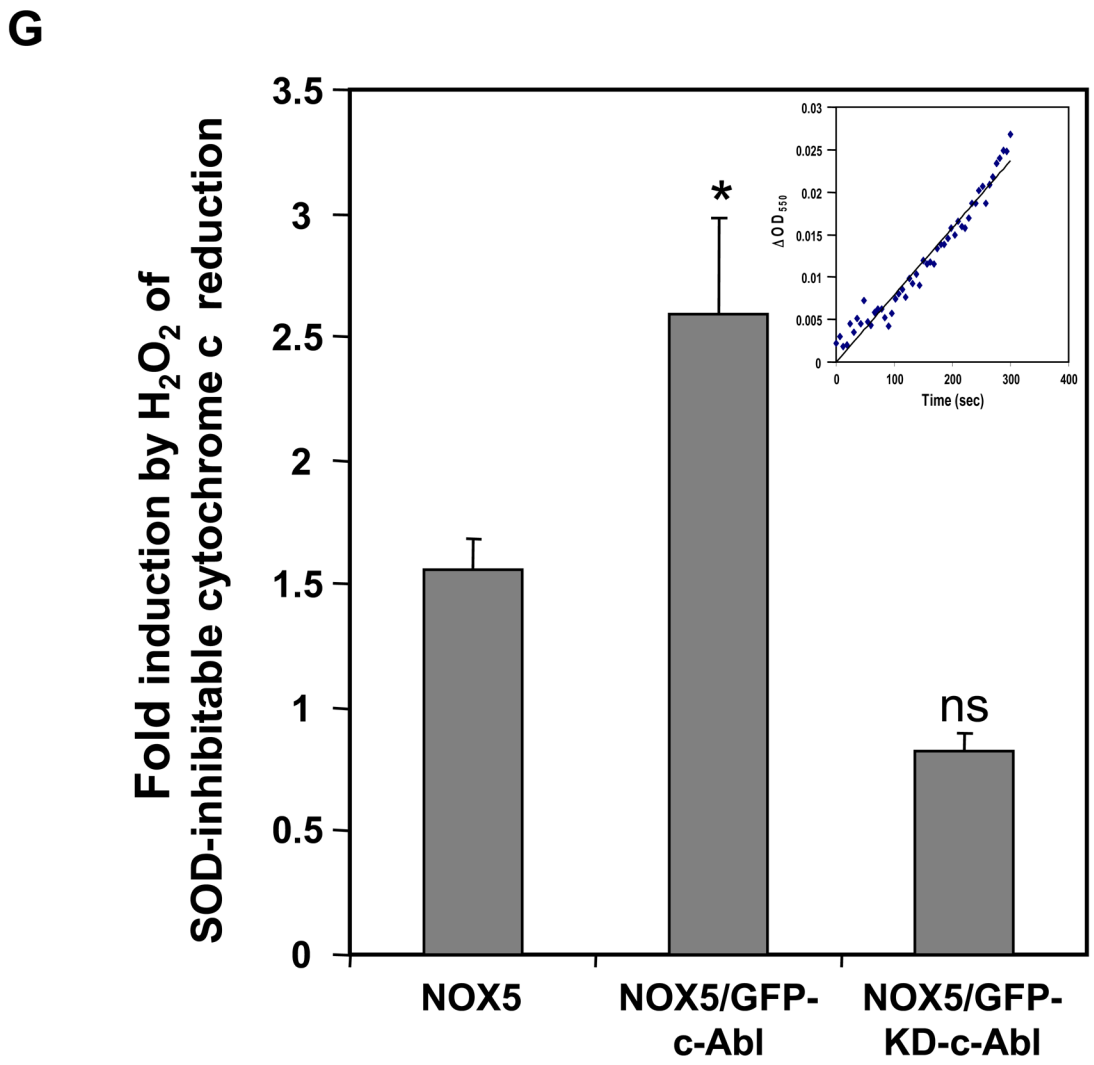

Fig. 8. Colocalization and functional interaction of wild type c-Abl with NOX5 activity in a cell-free assay

(A) Lysates from K562/NOX5 expressing either kinase-active GFP-c-Abl or the kinase-dead GFP-c-Abl, and treated with or without 100μM H_2O_2, were immunoprecipitated with anti-GFP as described in Fig. 7, and immunoblotted with antibodies to c-Abl and NOX5. (B) After densitometric analysis, the NOX5 protein content in the GFP-immunoprecipitates was determined and normalized to the corresponding GFP protein level. (C) Anti-c-Abl immunoprecipitates from the lysates of HEK and HEK/NOX5 cells were immunoblotted with antibodies to c-Abl and NOX5. **(**D) Immunoblots with antibodies to cAbl, NOX5, and PDI (loading control) were performed using crude membranes preparations from K562/NOX5 cells expressing GFP-c-Abl or GFP-KD-c-Abl and treated with or without H_2O_2.. E, F) After densitometric analysis, the levels of Abl proteins (GFP-Abl plus endogenous c-Abl proteins) and NOX5 proteins were normalized to the corresponding PDI protein levels and expressed as a percentage of the control value (100%) obtained from H_2O_2-untreated cells. Data are the mean +/− SEM of three independent experiments. (G) K562/NOX5 cells and K562/NOX5 cells expressing GFP-c-Abl or GFP-KD-c-Abl were treated with or without H_2O_2 (100 μM) for 10 minutes, then crude membranes were prepared and assayed for superoxide generation using SOD-inhibitable cytochrome c reduction. The data represent the H_2O_2-induced fold

increase in superoxide formation and are the means +/− SEM of 3–7 independent experiments. Asterisks indicate statistical significance versus the fold increase in NOX5 activity measured using K562/NOX5 cells. * $P < 0.05$ or ns. The inset in Fig. 8D is a representative cytochrome assay performed with membranes of untreated K562/NOX5 cells. The graph depicts the Δ 50nm absorbance as a function of time.

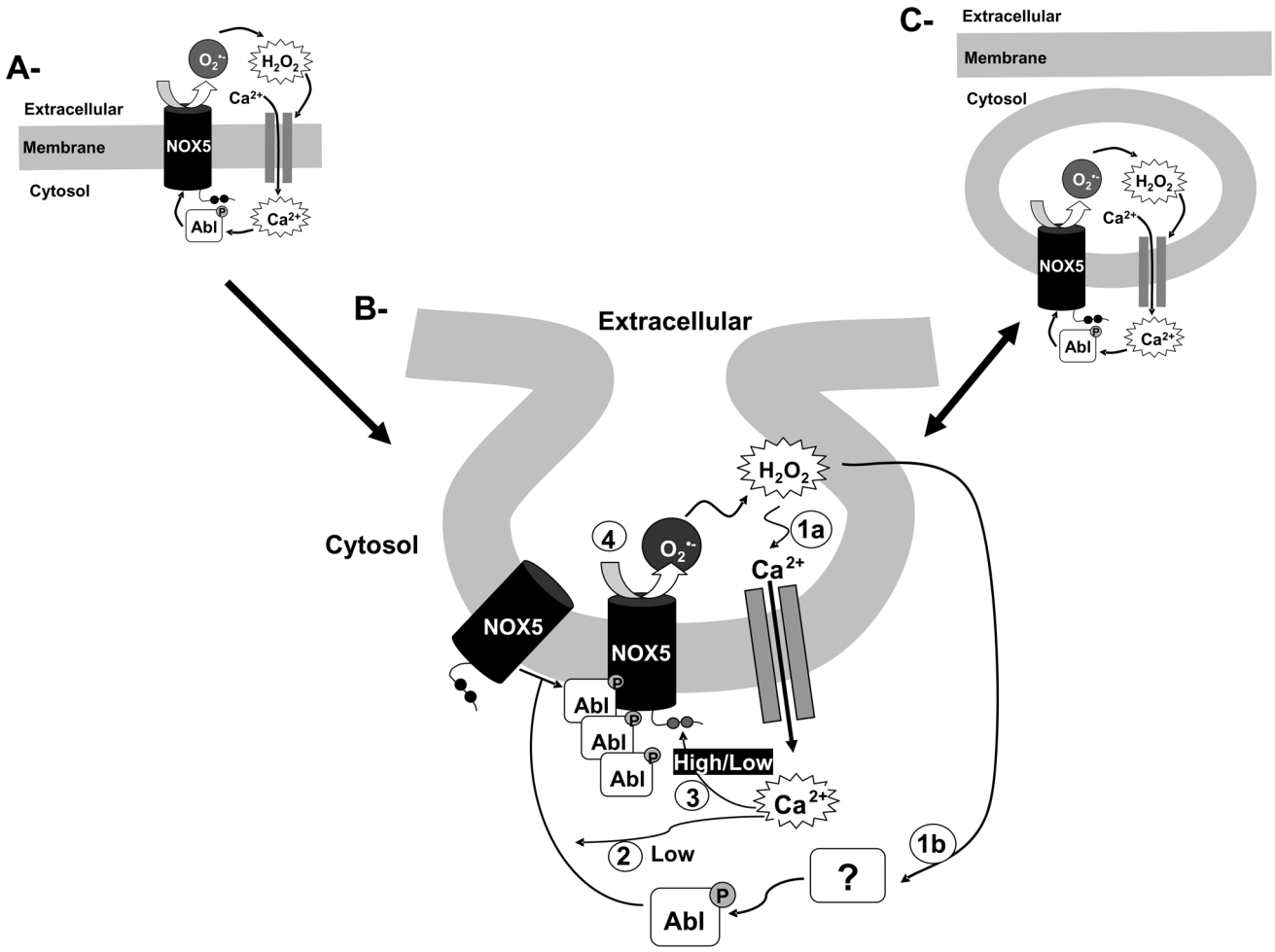

Fig. 9. Proposed model for H_2O_2-NOX5 regulation: the amplification loop

H_2O_2 induces simultaneously a low calcium influx (panel B, step 1a) and the activation of cAbl through tyrosine phosphorylation (panel B, step 1b). The low calcium influx and the activation of c-Abl are required for the translocation of c-Abl to the membrane (panel B, step 2). These events are accompanied by c-Abl oligomerization. The c-Abl oligomers through either a direct or indirect interaction with NOX5 stimulate its activity, possibly by enhancing its sensitivity to a low concentration of calcium (panel B step 3). Once NOX5 is activated, the generation of superoxide anion through its dismutation to hydrogen peroxide and/or through the formation of more highly reactive oxygen species then amplifies the primary signal (panel B, step 4). When a stimulus generates a high cytosolic calcium concentration (e.g. ionophore exposure), the stimulation of NOX5 is independent of c-Abl, and Ca^{2+} then directly activates NOX5. Along with this amplification loop there is evidence suggesting the compartmentalization of superoxide production, which occurs only at the plasma membrane and in discrete intracellular vesicular compartments networking with the plasma membrane (panel A, B and C and Fig. 5A). However, our results suggest that the initial event in this pathway is the production of superoxide at the plasma membrane.